ACS APPLIED MATERIALS & INTERFACES

www.acsami.org

Research Article

Structure–Function Correlations in the Mechanism of Action of Key Antiperspirant Agents Containing Al(III) and ZAG Salts

Arnab Dawn, Fred C. Wireko, Andrei Shauchuk, Jennifer L. L. Morgan, John T. Webber, Stevan D. Jones, David Swaile, and Harshita Kumari*

Cite This: *ACS Appl. Mater. Interfaces* 2022, 14, 11597–11609

Read Online

ACCESS | Metrics & More | Article Recommendations | Supporting Information

ABSTRACT: Aluminum hydrolysis chemistry is an important part of modern society because of the dominance of Al(III) as a highly effective antiperspirant active. However, the century-old chemistry centered on aluminum chloride (ACL) is not comprehensive enough to address all of the *in vivo* events associated with current commercial antiperspirants and their mechanism of action. The present study aims to address the knowledge gap among extensively studied benchmark ACL, its modified version aluminum chlorohydrate (ACH), and a more complex but less explored group of aluminum zirconium chlorohydrate glycine complexes (ZAG salts) toward understanding the mechanism of action under consumer-relevant conditions. ACH, which is the Al source used in the manufacture of ZAG salts, provides a bridge between ACL and ZAG chemistry. High viscosity and gel formation driven by pH and a specific Al(III) salt upon hydrolysis are considered the criteria for building an *in vivo* occlusive mass to retard or stop the flow of sweat to the skin surface, thus providing an antiperspirant effect. Rheological studies indicated that ACL and aluminum zirconium tetrachlorohydrex glycine (TETRA) were the most efficacious salt actives. Spectroscopic studies, diffraction studies, and elemental analysis suggested that small metal oxide and hydroxide species with coparticipating glycine as well as various polynuclear and oligomeric species are the key to gel formation. At a given pH, the key ingredients (NaCl, urea, bovine serum albumin, and lactic acid) in artificial sweat were found to have little influence on Al(III) salt hydrolysis. The effects of the sweat components were mostly limited to local complex formation and kinetic modification. The *in vitro* comparative experiments with various Al(III) and ZAG salt systems offer unprecedented insights into the chemistry of different salt types, thus paving the way for engineering more efficacious antiperspirant systems.

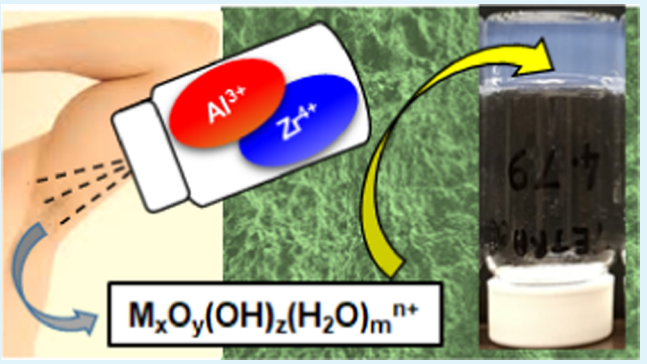

KEYWORDS: *aluminum hydrolysis, antiperspirant, ZAG salt, speciation, mechanism of action, structure–function correlation, hydroxide, gel*

INTRODUCTION

Aluminum is the third most abundant element in Earth's crust. Because of its widespread availability in soil and natural waters, its ability to interact with various ligands and water depending on pH, and its global use in many consumer-involved applications, the chemistry of Al(III) has been a topic of interest for over a century.[1−3] Al chemistry is used in various industrial applications including for coagulants in water purification treatment plants[4−7] and in clay pillaring.[8,9] The low pH of current commercial Al(III) salts provides strong antibacterial effects.[10,11] The toxicity of Al(III) salts to humans has also been well studied, especially in recent years, owing to the unfounded conclusion that topical treatment causes Al to be absorbed through the skin, leading to potentially serious health issues.[12−16] Although the scientific evidence supporting this claim has been shown to be unfounded, general chemophobia and the natural products movement continue to create a need for Al-free antiperspirant technologies.

Al(III) salts were first used in antiperspirants in 1903.[17,18] However, the highly acidic pH of the initial aluminum salt, aluminum chloride (ACL), led to skin irritation and clothing damage. Thereafter, a more buffered Al(III) salt, aluminum chlorohydrate (ACH), was used.[19] Extending such technology further, new salts such as aluminum zirconium chlorohydrate glycine complexes (ZAG salts) were designed by blending ACH with zirconyl chloride or zirconyl hydroxychloride in the presence of glycine. These salts, which were specifically developed for anhydrous formulations, have been found to be superior to ACH in terms of efficacy.[20,21]

Received: November 23, 2021
Accepted: February 8, 2022
Published: February 25, 2022

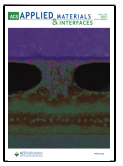

Antiperspirants are topically applied and limit eccrine sweat production. It is believed that the action of antiperspirants based on Al(III) and ZAG salts containing Zr(IV) ions depends on the formation of an occlusive plug of polycationic Al ions with polyanionic salts such as the amino acids, peptides, and proteins from sweat or even the ductal wall.[22−26] Irrespective of the mechanism of action, the formulation of Al(III)- and ZAG-salt-based antiperspirants largely relies on the fact that partially neutralized small Al and/or Zr species enhance the sensory profile of the product with the skin and maintain product efficacy. More recently, calcium ions combined with glycine have been added to the solutions of ZAG actives to stabilize Al species, which historically were only stable in solid antiperspirant actives. In industry, such hypotheses are frequently applied to optimize, within the FDA monograph, the speciation of Al(III) and Al(III)−Zr(IV) salt solutions via process conditions to achieve high antiperspirant efficacy.[27,28] However, there is still no clear evidence that correlates the formulation/process strategy with the mechanism of action and the *in vitro* efficacy/performance. The key reasons for this knowledge gap are the following: (i) challenges in mimicking ductal events during *in vitro* experiments, (ii) a poor understanding of Al hydrolysis events beyond simple ACL and ACH, especially in complex substrate environments such as with ZAG salts, and (iii) a lack of data for correlating *in vitro* experiments during the product formulation stage with the product application stage. In addition, because Al(III) hydrolysis events are pH sensitive, the performance of antiperspirant products will vary from consumer to consumer, as the pH of secreted sweat constantly changes depending on exertion and secretion rates or even the time of day.[29−32]

In an effort to address some of the above-mentioned issues, we report, for the first time, comprehensive and comparative studies on the *in vitro* hydrolysis events of five Al(III) salts that are widely used for antiperspirant formulation. The investigated Al(III) salts were the initial benchmark ACL, its modified version ACH, and three ZAG salts, namely, aluminum zirconium trichlorohydrex glycine (TRI), aluminum zirconium tetrachlorohydrex glycine (TETRA), and aluminum zirconium octachlorohydrex glycine containing calcium chloride (OCTA). The objective of this work was to obtain a comprehensive understanding of the behavior of each salt under consumer-relevant conditions, such as in artificial sweat versus water, under varying pH conditions, and at ambient temperature. Importantly, we explored whether such quantitative data could provide greater insights into the physiochemical/biophysical roles of Al(III) salts in antiperspirant performance.

One of the most intriguing aspects of Al hydrolysis is the complex nature of the hydrolysis products, which range from simple monomeric to highly polymeric Al species.[33−38] These hydrolyzed species are very sensitive to the local environment, especially to the pH of the medium.[39−41] Concentration, temperature, coexisting anions, and the base addition rate can also influence hydrolysis events.[42−45] In general, at low pH values (<3), Al^{3+} ions are coordinated by water molecules and exist as hydrated cations. As the pH value is increased by adding hydroxides (e.g., sodium, potassium, or ammonium hydroxide), the Al species are coordinated by hydroxides and protons are removed from the medium, with subsequent condensation of the hydroxide groups. This process eventually leads to the formation of larger colloidal species that trigger a sol−gel state, resulting in an increase in the viscosity of the medium or the generation of a phase-separated mass. When the OH/Al molar ratio is higher than 2.5, it is anticipated that various polyatomic Al species will interact with each other to form Keggin tridecamers, which have been extensively researched. One challenge in understanding such complex chemistry is the unambiguous detection of various Al species using available analytical techniques. For example, ^{27}Al NMR spectroscopy can detect only limited types of highly symmetric Al species.[38,46−49] In other words, other low-symmetry polymeric Al species may exist that cannot be detected using ^{27}Al NMR spectroscopy.[50,51] Therefore, the evaluation of Al chemistry has largely relied on cooperation among experimental findings, hypotheses, and various models.[3]

In this work, rheological measurements of various Al(III) and ZAG salts were used to compare their propensities for forming high-viscosity masses (e.g., a gel or precipitate). In addition, rheological measurements were performed for these salts in the presence of known key sweat ingredients (sodium chloride, bovine serum albumin (BSA), lactic acid (LA), and urea) to evaluate their impact on the formation of high-viscosity masses. Subsequently, parallel hydrolysis events were performed in the presence and absence of the sweat components. Finally, various structure−function relationships were investigated using spectroscopic techniques, X-ray diffraction, inductively coupled plasma optical emissions spectrometry (ICP-OES), and morphological studies. The intention of these *in vitro* studies using a simple setup was twofold. First, such studies can expand the chemistry of Al(III) hydrolysis beyond the benchmark ACL to more complex salt compositions and complex microenvironments, thus advancing academic knowledge. Second, such studies can reveal underlying chemistry that is beneficial to the antiperspirant industry for optimizing formulations toward the realization of superior efficacy.

EXPERIMENTAL SECTION

Materials. ACL was purchased from Sigma and all other salts (ACH, TRI, TETRA, and OCTA) were supplied by Procter & Gamble and used as received. ACH and OCTA were supplied as 50 and 30% solutions, respectively. Sodium chloride, urea, and LA were purchased from Fisher Scientific. BSA and ammonium hydroxide (NH_4OH) solutions were purchased from Sigma.

Preparation of Sweat Mimic (SM). Sodium chloride, BSA, urea, and LA were added to water so that the final concentration of each component was 0.4% (w/v).

pH Adjustment. Typically, in the first step, a 10% (w/v) Al(III) salt solution was prepared either in water or in the preprepared SM by adding an appropriate amount of an Al(III) salt to the required volume of water or SM. In the second step, the pH of the Al(III) salt solution was adjusted (increased) as required by adding 15% NH_4OH solution in 0.05 mL portions under stirring followed by vortexing for 10 s. pH measurements were performed using a Seven Compact pH/ion meter.

Xerogel Preparation. After hydrolysis (pH adjustment as described above) and subsequent ageing at room temperature for 20 h, 3.5 g of gel was added to 8 mL of water for 75 min. Subsequently, the liquid from the top was decanted carefully. The entire process was repeated a second time. The final gel mass was freeze-dried and then vacuum-dried for several hours to obtain the xerogel.

Rheological Measurements. Rheological measurements were performed 20 h after pH adjustment using a Discovery HR-2 rheometer. A 40 mm cone-plate steel geometry with 55 mm truncation was used for all experiments. Flow-ramp experiments

https://doi.org/10.1021/acsami.1c22771
ACS Appl. Mater. Interfaces 2022, 14, 11597−11609

Table 1. Theoretical Compositions of the Al(III) and ZAG Salts Used in the Study

salt	Al (wt %)	Zr (wt %)	Cl (wt %)	glycine (wt %)	Ca (wt %)	Al/Zr (mole ratio)	metal/Cl (mole ratio)	Zr/Gly (mole ratio)
aluminum chloride (ACL)	20.00		80.00				0.32	
aluminum chlorohydrate (ACH)[a]	12.50		8.47				1.91	
aluminum zirconium trichlorohydrex glycine (TRI)	18.30	10.90	16.80	10.60		5.67	1.65	0.80
aluminum zirconium tetrachlorohydrex glycine (TETRA)	14.68	13.75	20.10	13.25		3.61	1.19	0.80
aluminum zirconium octachlorohydrex glycine (OCTA)[a]	7.13	2.58	9.90	10.60	1.63	9.33	1.03	0.19

[a]ACH and OCTA were supplied as 50 and 30% aqueous solutions, respectively.

were performed by measuring the sample viscosity under varying shear rates between 5×10^{-4} and 30 s^{-1} at 25 °C.

Scanning Electron Microscopy (SEM). SEM and energy-dispersive X-ray spectroscopy (EDAX) were performed using a SCIOS SEM/FIB instrument (Thermo Fisher Scientific) equipped with an energy-dispersive X-ray system. A small amount of sample was deposited on a silicon wafer, freeze-dried by submersion in liquid nitrogen, and then dried in vacuo for 2 days. Before analysis, the samples were coated with palladium.

Fourier transform infrared (FT-IR) Spectroscopy. A Nicolet 6700 FTIR spectrophotometer with a Smart Orbit diamond ATR module was used to collect FT-IR spectra of the solid samples in the spectral range 4000−400 cm^{-1}.

Wide-Angle X-ray Scattering (WAXS). WAXS data were collected using a Stoe STADI-MP diffractometer. The generator was operated at 40 kV/40 mA, powering a long-fine-focus X-ray tube with a Cu anode. The diffractometer incorporated an incident-beam curved germanium crystal monochromator, a standard incident-beam slit system, and a Mythen PSD detector. Data were collected in transmission mode in the 2θ range 0−60° with a step size of 1° and a scan rate of 20 s/step.

ICP-OES. The samples were digested completely using a mixture of nitric and fluoroboric acids in a Milestone Ultrawave digestion system. The resulting digestates were diluted to a set volume using deionized water (18 MΩ·cm) after the addition of an appropriate internal standard solution (gallium). A method blank was also prepared, which contained all of the reagents but no sample, to assess potential process contamination. Predigestion spikes were prepared for select samples by fortification with a known level of an analyte. Working standards were prepared by combining appropriately diluted stock solutions of reference standards, covering the concentration range of interest, with the internal standard. The final composition of the prepared working standards was matched to the prepared samples in terms of acid content. The results from the ICP-OES analysis of these working standards were used to prepare a calibration curve for the quantitation of Al and Zr. For each analyte, the correlation coefficient of the calibration curve was >0.999. The prepared standards, test samples, and spiked samples were analyzed using an Agilent 5110 ICP-OES instrument. At least two wavelengths were used to demonstrate adequate selectivity, with one wavelength chosen for reporting purposes. The instrument was optimized according to the manufacturer's recommendations. Various quality control (QC) measures were implemented to ensure data quality, namely, the method blank was less than the lowest standard, the spike and recovery results for the fortified sample were between 87 and 102%, and the results for periodic QC reinjection of the standards were between 97 and 100%.

RESULTS AND DISCUSSION

Sample Preparation and Selection of Al(III) and ZAG Salts. In the current study, five different Al(III) salt systems were used (Table 1). ACL is used as a benchmark because it is the simplest system among the investigated salts. Compared with ACL, ACH has a higher Al/Cl ratio and is a partially neutralized Al(III) salt. All three ZAG salts contain Zr(IV) and glycine in addition to Al(III). Among the ZAG salts, OCTA and TETRA have the lowest and highest amounts of Zr(IV), respectively. Unlike the other ZAG salts, OCTA is obtained as an aqueous solution that also contains calcium chloride ($CaCl_2$). This compositional variety is beneficial for assessing the role of the Al/Cl ratio, Zr(IV), glycine, and Ca(II) in gel formation. To investigate the effect of sweat on salt hydrolysis, a simplified SM was prepared by adding four key sweat components (LA, NaCl, BSA, and urea) to water, each at a final concentration of 0.4% (w/v).[52] LA, NaCl, BSA, and urea can be considered as model substrates representing carboxylic ligands, inorganic salts, proteins, and neutral additives, respectively. The concentrations of the substrates were higher than their actual levels in eccrine sweat to facilitate the evaluation of their influence. Throughout this study, a total salt concentration of 10% (w/v) was maintained in the tested systems, which is a reasonable approximation of the *in vivo* concentration of salts when a commercial antiperspirant is applied and dissolved during sweat events. For the hydrolysis/pH adjustment experiments, NH_4OH was used instead of NaOH because ammonium ions are an integral component of eccrine sweat. Furthermore, this allowed a constant sodium level to be maintained throughout the experiments (no sodium in the case of water and a fixed sodium level for SM systems). To minimize the effect of external factors, a constant base addition rate and the same mixing/agitation methods were used throughout all hydrolysis experiments. All hydrolysis/pH adjustment experiments were performed at room temperature (~22 °C). After pH adjustment, the samples were kept undisturbed for 20 h before being subjected to rheological measurements and other characterization techniques. All of the studied systems had pH values in the range 4.00−7.00, which is similar to the pH range of eccrine sweat. Upon the periodic addition of NH_4OH during the hydrolysis experiments, the samples became opaque above a threshold pH, which varied depending on the salt system.

All of the systems formed highly viscous gels (evaluated by the stable-to-inversion method) above pH 6.00 (Figure 1), both in water and in the SM. ACL and TETRA also formed viscous gels below pH 5.00, although the behavior of these two systems differed. ACL gained significant viscosity (by appearance) starting at pH 4.50 and exhibited consistency throughout the pH range. In contrast, TETRA showed a sudden viscosity increase and gel formation in a narrow pH range (4.50−5.00). In addition, TETRA gelling at pH < 5 occurred slowly over time.

Hydrolysis experiments in water are beneficial for revealing the key underlying chemistry and for differentiating between benchmark ACL and more complicated systems. Furthermore, performing parallel experiments in the SM can clarify the

https://doi.org/10.1021/acsami.1c22771
ACS Appl. Mater. Interfaces 2022, 14, 11597−11609

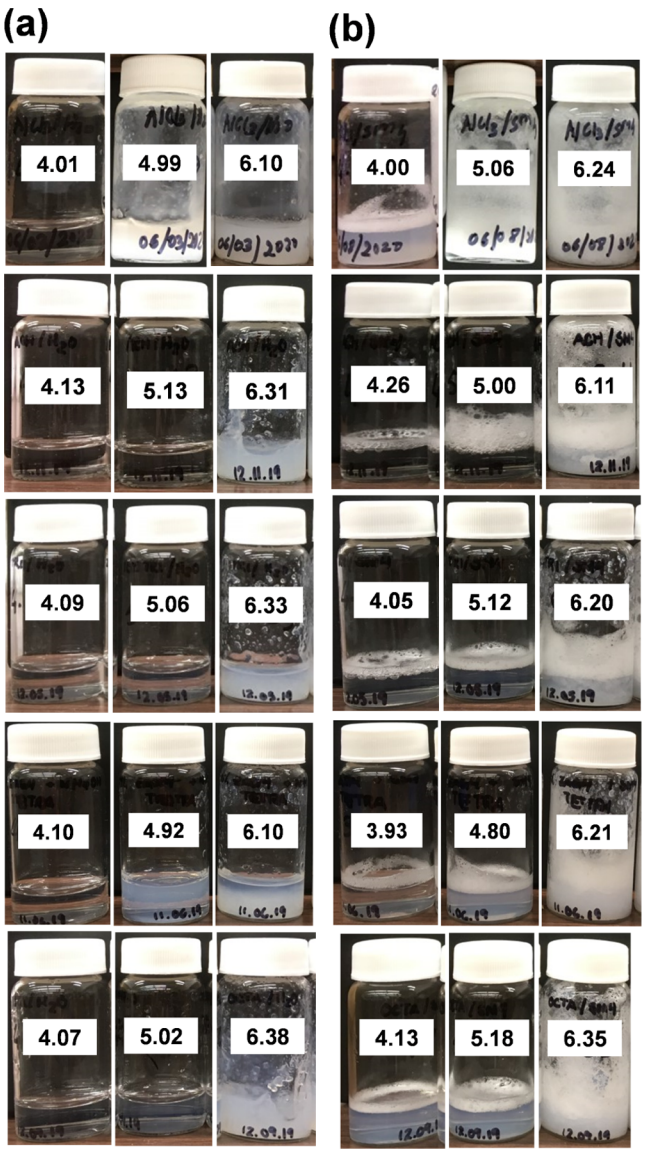

Figure 1. Photographs (at selective pHs) of various samples (10% w/v) of ACL, ACH, TRI, TETRA, and OCTA (top to bottom) salts prepared by adjusting pH as mentioned and after 20 h of aging at room temperature: (a) in water and (b) in SM.

influence of sweat substrates on hydrolysis chemistry. Any differences in system behavior and physicochemical properties can be directly related to the influence of the SM components. The solution systems in the SM, especially at low pH values, appeared cloudy, whereas transparent systems were observed in water. Furthermore, the gels formed in the SM were more opaque than the gels formed in water. Such differences could be related to the presence of various SM components and the formation of local complexes with the metals.

Rheological Measurements. High viscosity and gel formation in a system are considered key factors that are indicative of favorable conditions for occlusive layer formation, which is necessary for the action of these salts as antiperspirants. Furthermore, the dependence of the viscosity of material on the rate at which it is sheared provides valuable information about processing and performance. The various gel systems prepared from 10% (w/v) Al(III) and ZAG salts upon pH adjustment were subjected to flow-ramp experiments (SI, Figures S1–S5). In this experiment, low shear rate behavior can be related to the properties of the material developed during the hydrolysis of the applied salts in the presence of a sweat current (at a specific local pH) upon application of an antiperspirant product. Therefore, the viscosity values obtained at near-zero shear rates (SI, Figures S1–S5) in water and in the SM are plotted in Figure 2. The

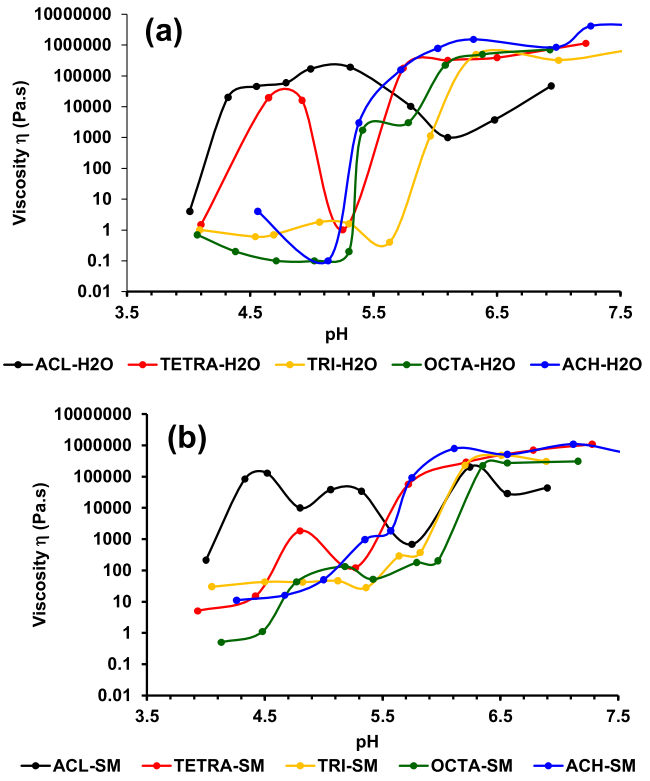

Figure 2. Viscosity profiles of 10% (w/v) Al(III) and ZAG systems (a) in water and (b) in the SM as a function of pH, as obtained using flow-ramp experiments.

pH vs viscosity plots (Figure 2) reveal key trends based on the salt type and the final pH of the system. Control experiments were conducted in water to allow the contributions of the Al(III) salt components and the sweat components to be assessed separately. The nature of the pH vs viscosity plot is crucially dependent on the speciation chemistry of Al(III) and/or Zr(IV) owing to metal hydrolysis at different pH values. Therefore, comparisons of the observed trends should allow the speciation chemistry of the associated systems to be evaluated as the function of salt type and pH.

In both water and the SM, most of the systems only exhibited a substantial increase in viscosity above pH 5.5. However, ACL and TETRA were exceptions, exhibiting increases in viscosity below pH 4.5. Therefore, under the present conditions, all of the other systems are unlikely to form *in vitro* occlusive masses below pH 5.5. However, all systems exhibited very high viscosity ($\sim 10^5$ Pa·s) and strong gel formation above pH 6. Thus, above this threshold pH, all of the systems are expected to form effective occlusive masses. The systems show differing behavior in the pH range 4–6. Therefore, to obtain a thorough understanding of the relevant chemistry, viscosity profiles were investigated in water, where the influence from SM components is absent. A sudden change in viscosity represents a change in either metal speciation or

https://doi.org/10.1021/acsami.1c22771
ACS Appl. Mater. Interfaces 2022, 14, 11597–11609

the superstructure of the assembled species or a combination of both.

For the benchmark ACL system in water, the viscosity did not exhibit abrupt changes, with the exception of some fluctuations in the pH range 5.5−6.5. As the speciation chemistry of ACL has been well studied, we attempted to understand the speciation behavior of other underexplored or unexplored salts based on ACL chemistry. The Al concentration in the ACL solution used for investigating the hydrolysis event was ∼0.8 M, which is in a range where the concentration dependency of speciation is less pronounced.[45,53] Other than pH, the key factor driving Al speciation is the [OH]/[Al] mole ratio. Therefore, we plotted viscosity profiles in water against the [OH]/[Al] ratio (Figure 3). In the current study, the [OH]/[Al] ratio was varied in the

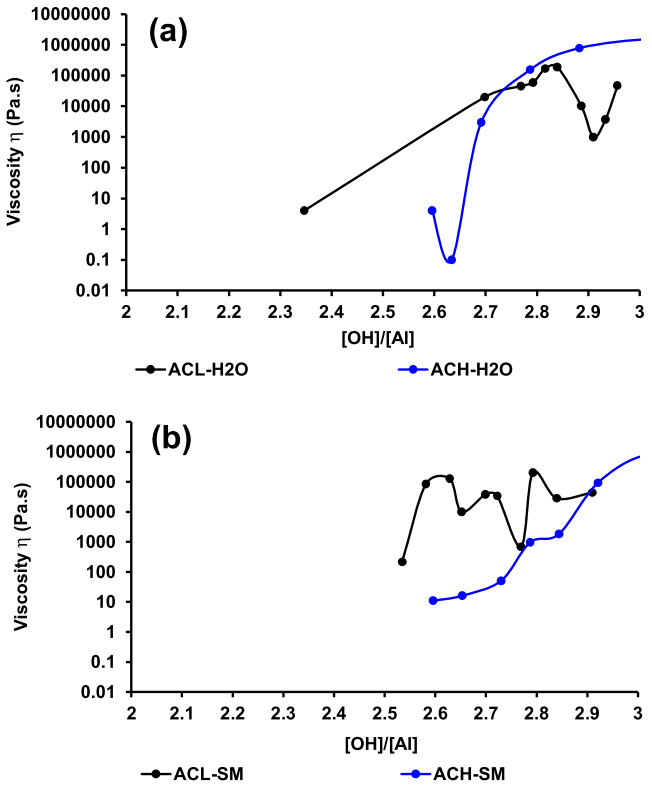

Figure 3. Viscosity profiles of 10% (w/v) ACL and ACH (a) in water and (b) in the SM as a function of [OH]/[Al] (mole ratio) (for ACH, [OH] is the total amount, i.e., the sum of the amount already present in ACH and the amount added during hydrolysis/base addition experiments).

range 2.3−3.0. Various models have previously been used to understand and address Al speciation. Without adhering to a particular model, it is expected that the ACL solution will be dominated by polynuclear species and aggregated polynuclear species in the tested pH range.[54] However, most speciation events cannot be detected/captured using ^{27}Al NMR spectroscopy. The very small change in pH during the initial stage of base addition to ACL indicates the binding of OH^- to Al^{3+} until a threshold point ([OH]/[Al] > 2.0) is reached. In general, at this point, the Al-tridecamer and other polynuclear species are expected to be dominant. In addition, during this phase, there was very little to no change in viscosity. After this stage, the system slowly transforms from a suspension to a soft gel at [OH]/[Al] > 2.3, and the pH of the medium increases rapidly and more consistently with the periodic addition of the base. This behavior indicates that the added OH^- ions are now free in solution instead of being bound to Al. In the present study, the onset of gelation occurred at [OH]/[Al] ∼ 2.69, which is in close agreement with previously reported results for an aluminum hydroxide gel.[55] In line with that report, it is reasonable to consider the formed gel to be a highly random structure containing polynuclear hydroxyaluminum species with a wide range of values for hydroxide bound to Al.[56] The formation of the polynuclear hydroxyaluminum body is considered to be a stepwise process involving a deprotonation−dehydration mechanism. The fluctuations in viscosity above [OH]/[Al] ∼ 2.69 in water can be attributed to such a random (amorphous) structured system.

In this study, the only other Al(III)-only system was ACH, which is partially neutralized and therefore less acidic than ACL. ACH (Table 1) is a basic aluminum chloride with the chemical formula $Al_2(OH)_5Cl$.[57,58] This material is expected to be dominated by aluminum polyoxo species, including Al_{30}-mer and Al_{13}-mer.[59] Therefore, unlike ACL, ACH shows a steady increase in pH from the very beginning of the hydrolysis experiment with a much lower amount of added base. In water, the ACH system forms a gel with a very high viscosity (>10^5 Pa·s) at [OH]/[Al] > 2.75. This value is close to that for the onset of ACL gelation, which might indicate a similar gelation pathway for ACH via hydroxide formation. The conversion of ACH to aluminum hydroxide has previously been explained by the dissociation of charged polynuclear aluminum upon neutralization via base addition up to a value [OH]/[Al] > 3.[60] Similarly, small intact Al_{30}-mer clusters and smaller Al species can undergo condensation reactions to produce larger clusters.[61] Therefore, in the present study, at 2.75 < [OH]/[Al] < 3, a transition phase is expected, in which clustered polynuclear aluminum coexists with aluminum hydroxide (discussed further in a later section).

The presence of Zr(IV) in addition to Al(III) in TRI, TETRA, and OCTA is expected to influence the degree of polymerization and hydrolysis significantly. Because Zr(IV) has a higher acidity and a greater affinity for OH^- than Al(III), it is much more challenging to assess the basicity of the Al(III) fraction in the presence of Zr(IV). Therefore, speculation about Al speciation based on only the [OH]/[Al] ratio is no longer useful. To obtain a better understanding of Al speciation, we measured the pH of the aqueous solutions of various salts before base addition (Table 2). These pH values

Table 2. Initial pH (before Base Addition) of 10% (w/v) Salts in Water and in the SM at 22 °C

	ACL	ACH	TRI	TETRA	OCTA
pH in water	2.56	4.13	3.68	3.37	3.76
pH in SM	2.07	3.96	3.70	3.21	3.62

should reflect the acidity of Al at the beginning of the hydrolysis event. As expected, ACL and ACH were the most acidic and most basic salts, respectively. Therefore, it is reasonable to expect intermediate Al speciation chemistry for TRI, TETRA, and OCTA. These ZAG salts were prepared by adding ACH and varying amounts of zirconium oxy- or hydroxychloride. Because of the highly acidic nature of the Zr(IV) salt, the resulting Al(III)−Zr(IV) salts are more acidic than ACH. These mixed salts are usually further buffered with glycine. In acidic solution, ACH hydrolyzes to form

https://doi.org/10.1021/acsami.1c22771
ACS Appl. Mater. Interfaces 2022, 14, 11597−11609

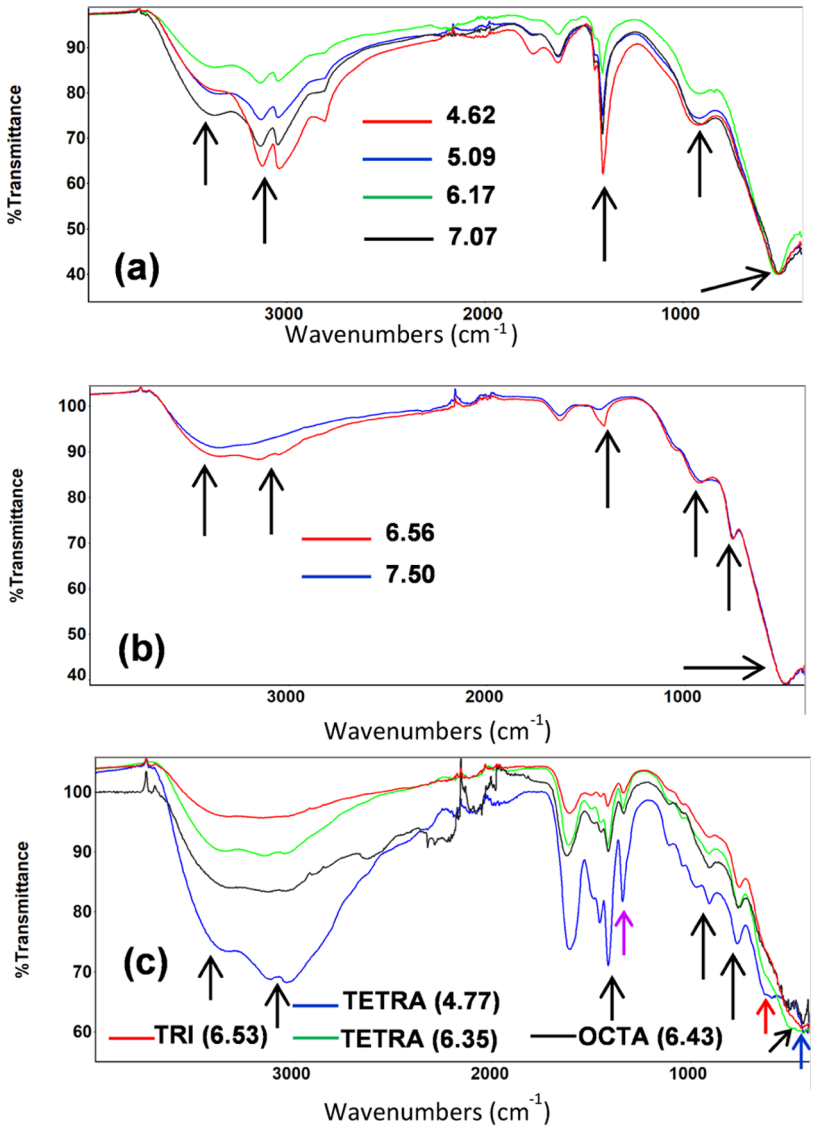

Figure 4. FT-IR spectra of xerogels (prepared after gel washing) of 10% (w/v) Al(III) and ZAG salts prepared in water at the shown pH values: (a) ACL, (b) ACH, and (c) TRI, TETRA, and OCTA (the colored arrows indicate the additional signals observed for the ZAG salts).

monomeric Al species, with the extent of this process depending on the Al/Cl ratio and the solution pH.[58] Among the Zr(IV)-containing salts, TETRA is the most acidic and is therefore expected to form the highest amount of monomeric/small Al species. Unlike the other ZAG salts, TETRA exhibits a high viscosity at pH < 5, which can be correlated with the initial presence of monomeric Al and its subsequent hydrolysis, similar to the path followed by ACL. However, the viscosity of TETRA decreases sharply above pH 5.0 and then increases again at pH > 5.5, similar to all of the other salts. Therefore, this unique behavior cannot be explained based on Al speciation alone, and contributions from Zr speciation and the influence of glycine cannot be ruled out at this stage. TRI and OCTA are more basic than TETRA and are therefore expected to involve lesser amounts of monomeric/small Al species at the beginning of hydrolysis. Neither of these salts show any viscosity increase/gel formation below pH < 6, and their viscosity profiles are more similar to that of ACH. TRI only forms a gel at pH 6.33, which is the highest value among the salts investigated in this study. This behavior could be related to TRI containing a smaller amount of Zr than TETRA. The acidity of OCTA falls between those of TETRA and TRI, as does its pH profile. Interestingly, OCTA also exhibits an additional "break" in the pH vs viscosity profile around pH 5.5. Although the origin of this behavior is not fully understood, it could be related to the participation of calcium ions, which are only present in OCTA. Otherwise, OCTA, which has the lowest level of Zr(IV), behaves similar to ACH, confirming the influence of Zr(IV) in the other ZAG salts.

In the SM, the differences in the behaviors of the salts with pH are less distinct than in water. In other words, the presence of sweat additives has some leveling effect. For example, as in water, the viscosity of TETRA in the SM increases significantly around pH 5. However, the magnitude of the viscosity is less in the SM than in water, indicating that the presence of SM components inhibits the formation of self-assembled species/clusters, as hypothesized above. Furthermore, the viscosity of OCTA is significantly lower in the SM than in water below pH 6. Therefore, SM components appear to have a more drastic effect on the behavior of OCTA than on that of any of the other Al(III) salts. The leveling effect of the SM is particularly notably below pH 5.5, whereas at higher pH values, there are

https://doi.org/10.1021/acsami.1c22771
ACS Appl. Mater. Interfaces 2022, 14, 11597−11609

only small differences between the viscosity values in the SM and in water. At lower pH values, the local formation of various complexes between the metals and the SM components may influence the speciation chemistry to some extent. However, at higher pH values (high [OH]/[Al] ratios), where the speciation chemistry is driven by hydroxide formation, the formation of these local complexes is unfavorable.

The findings from the pH vs viscosity studies are fourfold: (i) all of the tested salts exhibit high viscosity and gel formation above pH 6, irrespective of the hydrolysis media (water or the SM); (ii) high viscosity and gel formation may be driven by Al speciation chemistry, which tends toward hydroxide formation, as in the cases of ACL and ACH, whereas the hydrolysis chemistry of the ZAG salts follows a somewhat intermediate path between ACL and ACH based on salt acidity and the presence of Zr(IV); (iii) although Zr speciation remains unclear, a complex scenario in which Zr(IV) coparticipates with Al(III) is highly probable; and (iv) the presence of SM components has a leveling effect on salt viscosity, but this influence is limited to low pH values.

FT-IR Study. FT-IR spectroscopy was used to investigate the xerogels of various Al(III) and ZAG salts to obtain a better understanding of the speciation chemistry (Figure 4). All of the gels were washed before forming the xerogels to eliminate any soluble components that might not be involved in the formation of the core structure. First, the FT-IR spectra of the Al(III)-only samples (ACL and ACH) were compared (Figure 4a,b). The broad peaks near 3400 cm^{-1} correspond to the stretching vibration of hydroxide directly bound to Al(III) (i.e., Al−OH).[35,62] The broad signal indicates a lack of ordering, which is reasonable because it is known that aluminum hydroxide gels must be aged for a very long time to induce a high degree of ordering, thus creating a nearly crystalline system.[63] No significant changes occur with increasing pH, other than an increase in the relative intensity, consistent with the addition of hydroxide. The signals in the range 3100−2800 cm^{-1} are ascribed to the O−H stretching vibrations of Al in an octahedral configuration (i.e., $Al(H_2O)_6$). These signals are particularly prominent for ACL, especially at lower pH values, and their relative intensities decrease as the pH increases, indicating the periodic replacement of water with hydroxides. In the case of ACH, the bands are much broader and nearly disappear above pH 7, signifying the involvement of more polymeric Al species than in the case of ACL. The band near 900 cm^{-1} is associated with the deformation vibration of hydroxyls bound to Al(III) (A1−O−H or Al−OH−A1). The presence of a distinct $(Al\text{-}OH_2)_{Oh}$ (octahedral) band near 500 cm^{-1} signifies the absence of very large polymeric Al species for all of the ACL gels prepared in the pH range 4.62−7.07.[64] Similarly, the observation of a relatively weak band for ACH indicates the presence of larger polymeric species. There are two additional distinct differences between the ACL and ACH spectra. First, for ACL, a strong signal is observed at ∼1400 cm^{-1}, even after gel washing. This signal is associated with NH_4Cl (formed by the reaction between added NH_4OH and Cl^- present in the Al(III) salt) and indicates its binding to the structure forming unit. The corresponding signal is negligible for ACH, suggesting the absence of NH_4Cl. Second, the Al−$O-Al_{Oh}$ (octahedral) band at ∼750 cm^{-1} is only present in the case of ACH.[65]

The FT-IR spectra of ZAG salts show all of the signals observed for ACH as well as a few additional signals, indicating the presence of similar Al species. For ZAG salts, the broad peak near 3400 cm^{-1} is expected to also include the stretching vibration of Zr−OH.[66] Similar to ACL, signals in the range 3100−2800 cm^{-1} are only prominent for TETRA at pH 4.77. This behavior indicates the presence of small Al species at low pH values, which is reasonable considering that TETRA has the highest acidity among the investigated ZAG salts. The distinct band at 650 cm^{-1} (indicated by a red arrow in Figure 4c), which is only observed for TETRA at pH 4.77, is ascribed to Zr−OH. The signal at 470 cm^{-1} (indicated by a blue arrow in Figure 4c), which is present for all of the ZAG salts, is associated with Zr−O−Zr stretching.[67] Another significant feature of ZAG salts is the glycine signal at 1300 cm^{-1} (indicated by a purple arrow in Figure 4c), which implies that glycine is bound to the structure after gel washing, likely via complexation with Al(III) and/or Zr(IV). Therefore, glycine might have an important role in gel formation for ZAG salts.

The FT-IR spectra of the xerogels of the Al(III) and ZAG salts prepared in the SM (SI, Figure S6) are not significantly different from those of the xerogels prepared in water. Therefore, SM components have a minimal influence on metal speciation, other than modifying the kinetics, as revealed by the rheological studies.

Based on the FT-IR spectra of Al and ZAG salts, the following conclusions can be drawn: (i) small metal species (i.e., low-molecular-weight species) are present in ACL and TETRA gels at low pH values, and these species are expected to be crucial for gel formation, as these are the only two systems that form gels at pH < 5; (ii) hydroxides are present in all gel systems; (iii) large to very large Al polymers are absent from the ACL gel, even at high pH values; (iv) NH_4Cl is bound to the ACL gel; (v) the presence of a unique Zr−OH signal for the TETRA gel at low pH values indicates that Zr is involved in gel formation; and (vi) sweat components used in the study do not participate in or influence gel formation.

WAXS Study. X-ray diffractograms of xerogel samples (after gel washing) prepared in water and in the SM indicate that the systems are mostly amorphous, as evidenced by broad signals in the 2θ range 4−7° (Figure 5). The associated sizes (Table 3) are much larger than the sizes of crystalline bodies reported in the literature.[58,63,65] The only crystalline signals observed are those of NH_4Cl, particularly for the ACL xerogel, which is consistent with the FT-IR results. Therefore, the diffraction signals of the current xerogels are expected to correspond to clusters or assemblies consisting of various Al and/or Zr species. The very similar sizes of these clusters signify that the salts have similar compositions. The structured species in the ACL xerogel are the same throughout the tested pH range and are independent of the hydrolysis media. The amorphous nature is further enhanced at higher pH values. Thus, increasing the pH may also widen the distribution of Al species, resulting in reduced order.

In the case of ACH, the SM affects not only the size but also the structural ordering. The ACH cluster could be smaller in water because large polymeric species are present with fewer small Al species, which are essential for cluster formation. The origin of the increased ACH cluster size in the SM is not fully clear. Among the ZAG salts, TETRA and OCTA xerogels formed at pH > 6 show the same cluster size as ACL, whereas the TRI xerogel contains somewhat larger species. The pH effect is prominent in the case of TETRA xerogels, with a smaller species observed at pH 4.77. Consistent with the unique signal in the FT-IR spectrum, this species might

https://doi.org/10.1021/acsami.1c22771
ACS Appl. Mater. Interfaces 2022, 14, 11597−11609

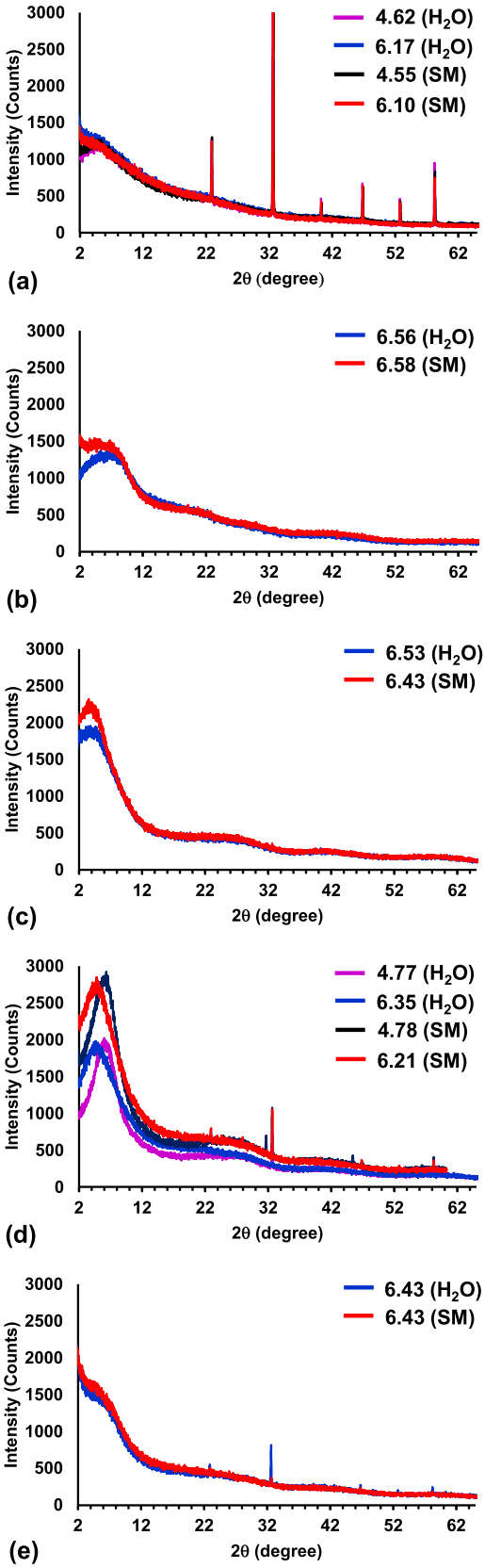

Figure 5. WAXS patterns of xerogels (prepared after gel washing) of Al(III) and ZAG salts: (a) ACL, (b) ACH, (c) TRI, (d) TETRA, and (e) OCTA. For each gel, the pH value is shown and the medium is given in parentheses.

indicate that the TETRA xerogel has a different composition at lower pH values, in which Zr(IV) is more involved. There are also noticeable differences in the extent of structural ordering. The TETRA xerogel at low pH appears to have the highest ordering, whereas ACL and OCTA xerogels are the least ordered. The incremental formation of amorphous hydroxides at higher pH values may suppress cluster ordering. However, the observation of comparable cluster sizes for all of the Al(III) and ZAG xerogels indicates that the clusters formed via the coparticipation of various Al and/or Zr species have similar compositions.

Structure–Function Relationships in Al(III) and ZAG Salts. The above characterization results for Al(III) and ZAG salts reveal that pH is the most crucial factor driving metal speciation and subsequent association processes. However, the hydrolysis temperature and aging time are also key factors. A high temperature and long aging time are beneficial for maximizing the conversion of a metal from one species to another. Furthermore, a long aging time facilitates the ordering of a particular species or its superstructure.[45] Therefore, in the literature, high temperatures (>80 °C) and long aging times (several days) have been used to isolate and identify various polymeric species. In contrast, in an effort to mimic the antiperspirant working mechanism under consumer-relevant conditions, room-temperature hydrolysis (~25 °C) and a short aging time (<24 h) were used in the present study. The adopted experimental conditions have two main effects that make evaluating metal speciation more challenging. First, the distribution of species is widened by incomplete/partial conversion. Second, the lack of ordering in the end product results in mostly amorphous systems.

In the present study, the observed changes in viscosity in conjunction with the metal/hydroxide ratio offer valuable insights into the Al speciation chemistry. Scheme 1 summarizes the information gathered about Al speciation, mostly based on ACL hydrolysis, which includes most of the events applicable to ACH and even ZAG salts. $Al(H_2O)_6^{3+}$ is representative of highly acidic ACL under pH-unadjusted conditions at the beginning of the hydrolysis event (phase-1). Upon base addition, the binding of OH^- and Al^{3+} with sequential replacement of H_2O occurs (phase-2). At [OH]/[Al] > 2.0, Al-tridecamer and other polymeric species are expected to dominate (phase-3). Until this point, no noticeable viscosity change is observed, which indicates the presence of soluble species. However, the rapid increase in viscosity at [OH]/[Al] > 2.3 indicates cluster formation with the existing species. As the FT-IR results ruled out the presence of very large polymers, the coassembly of small and moderately large Al species (no more than Al_{30}-mer) is anticipated. Finally, at [OH]/[Al] > 2.7 (phase-4), where the viscosity of the system is the highest, polynuclear hydroxyaluminum species with a wide range of values for hydroxide bound to Al are expected to be dominant. It is important to note that because small and large species coexist in almost all of these phases (this wide distribution is the result of incomplete conversion at room temperature within 20 h), cluster formation and subsequent gelation become feasible with relatively less-ordered (amorphous, as evidenced by WAXS) superstructures, avoiding the formation of a crystalline precipitate. The formation of small colloidal particles of aluminum hydroxide linked together to form an open, tenuous fractal structure has been reported.[45,68] Interestingly, the diameters of the subunits in the fractal network obtained from small-angle neutron scattering experi-

https://doi.org/10.1021/acsami.1c22771
ACS Appl. Mater. Interfaces 2022, 14, 11597−11609

Table 3. Sizes of the Repeating Units (in nm) in the Xerogel Samples (Prepared after Gel Washing), as Calculated from the WAXS Data[a]

media	ACL	ACH	TRI	TETRA	OCTA
water	1.8 (4.62)	1.3 (6.56)	2.0 (6.53)	1.5 (4.77)	1.8 (6.53)
	1.8 (6.17)			1.8 (6.35)	
SM	1.8 (4.55)	1.9 (6.58)	2.2 (6.43)	1.5 (4.78)	1.8 (6.43)
	1.8 (6.10)			1.8 (6.21)	

[a]The associated pH values are given in parentheses.

Scheme 1. Proposed Al Speciation at Various Stages of Base Addition

$$Al(H_2O)_6^{3+} \rightleftharpoons Al_{x1}(OH)_{y1}(H_2O)_{z1}^{(3x1-y1)+} \rightleftharpoons Al_{x2}O_m(OH)_{y1}(H_2O)_{z1}^{(3x2-2m-y1)+} \rightleftharpoons Al_{x3}(OH)_{y3}^{(3x3-y3)+}$$

([OH]/[Al] < 2) (2 <[OH]/[Al] < 2.7) ([OH]/[Al] > 2.7)

Phase-1 Phase-2 Phase-3 Phase-4

ments are in the range 1−2.5 nm, which is consistent with the d-spacing values determined from the WAXS data for xerogel samples. Therefore, in the present systems, similar fractal growth could lead to the formation of larger clusters and sol−gels.

Because ACH is more basic, phase-1 and phase-2 are absent. In addition, at the beginning of the hydrolysis event of ACH, presence of small Al species are less, as ACH is dominated by Al_{13}-mer (and Al_{30}-mer). However, polynuclear Al in ACH undergoes partial dissociation upon base addition and subsequent charge neutralization, forming smaller bodies, which trigger the formation of larger clusters by condensation and coassembly. Although gel formation via hydroxide formation in phase-4 is very similar for ACL and ACH, for the latter, large polymeric Al species are involved, as revealed by the FT-IR results for the ACH xerogel.

The Al speciation in ZAG salts is even more complicated. First, the acid hydrolysis of ACH in the presence of Zr forms smaller species by depolymerization. Second, acid-hydrolyzed ACH can then undergo base hydrolysis. Because TETRA has the highest acidity among the ZAG salts, it is expected to contain substantial amounts of small Al species at the beginning of base hydrolysis. This event is less pronounced for less acidic TRI and OCTA. Therefore, it is reasonable to consider the Al speciation chemistry in the ZAG salts to lie between those in ACL and ACH, with TETRA being more similar to ACL. Morphological investigations revealed irregular superstructures dominated by spherical particles (SI, Figures S7−S9), except for the TETRA xerogel at low pH, which exhibited a more interpenetrating morphology (SI, Figure S8).

Further, for ZAG salts, to understand the involvement of Zr(IV) and glycine in gel formation, washed gel samples (the same samples as used for FT-IR and WAXS measurements) prepared in water at various pH values were characterized using ICP-OES and C,H,N analysis (Table 4). It is worth noting that the TETRA xerogel at the lower pH value has a smaller Al/Zr ratio than the TETRA xerogel at the higher pH value, which indicates the greater involvement of Zr(IV) at low pH values. Further, EDAX elemental mapping of the TETRA xerogel at the lower pH value revealed a uniform distribution of Al and Zr, without any visible microphase separation (Figure 6). Collectively, these findings indicate the favorable coassembly of Al(III) and Zr(IV), with the Al speciation in phase-2 or even phase-3 (Scheme 1). Interestingly, for TETRA xerogels, the relative amount of glycine (calculated based on carbon analysis) is greater at the lower pH value (Table 4).

Table 4. ICP-OES and Elemental Analysis Results for Xerogel Samples Prepared (after Gel Washing) from ZAG Salts at Various pH Values (All Values Are Approximated to One Decimal Place)

system (pH)	Al (wt %)	Zr (wt %)	Al/Zr (mole ratio)	C (wt %)	Gly (wt %)	Al:Zr:gly (mole ratio)
TRI (6.53)	16.2	16.4	3.3	3.3	10.3	4.4:1.3:1
TETRA (4.77)	13.2	14.4	3.1	4.2	13.0	2.8:0.9:1
TETRA (6.35)	15.0	14.5	3.5	3.6	11.2	3.7:1.1:1
OCTA (6.43)	16.0	5.6	9.7	2.7	8.4	5.3:0.6:1

This observation indicates that metal−glycine complex formation is favorable at low pH values,[69−72] whereas metal/OH^- interactions may become more favorable at higher pH values. The retention of glycine in xerogels (based on the composition of the source salts as given in Table 1) is the highest for TETRA at the lower pH value and significantly smaller for OCTA and TRI. Because TETRA has the highest acidity among the tested ZAG salts, glycine retention could be due to the formation of complexes with small metal species and subsequent cluster formation.[73] This behavior would also reasonably explain the absence of gel formation in less acidic TRI and OCTA. Therefore, the sharp change in TETRA viscosity and the occurrence of gel formation below and above pH 5.5 (Figure 2) could be explained by a switch from metal/glycine coassembly to metal (hydroxide)-driven assembly, similar to all of the other salts above pH 6. The slow formation of a less amorphous TETRA gel at pH 4.77 indicates the growth of an ordered body, whereas an amorphous gel was quickly formed at pH > 6. Therefore, the unique gelation behavior of TETRA at low pH values (4.5−5.0) can reasonably be attributed to the collective contributions from small Al and/or Zr species and subsequent complexation with glycine. At high pH values with a high [OH]/[Al] ratio, metal−hydroxide coordination is expected to be predominant over metal−amino acid binding. Interestingly, the involvement of Zr at pH > 6 is particularly prominent for TRI, where the Al/Zr ratio in the xerogel (Table 4) is substantially lower than that in the source salt (Table 1). This behavior may be related to Zr(IV) having a greater hydroxide formation capacity than Al(III).

In contrast, the various components in the SM did not significantly influence the hydrolysis chemistry of the salts. The formation of local complexes between the SM components and

https://doi.org/10.1021/acsami.1c22771
ACS Appl. Mater. Interfaces 2022, 14, 11597−11609

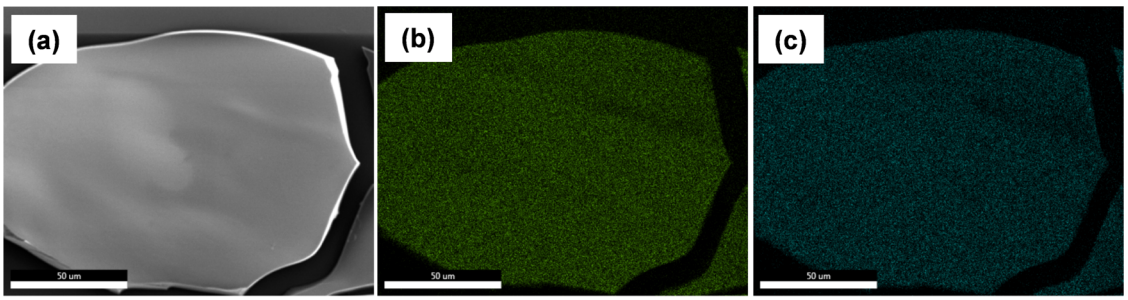

Figure 6. EDAX elemental mapping of the TETRA xerogel prepared in water at pH 4.86 (after gel washing): (a) SEM image of the sample, (b) Al mapping, and (c) Zr mapping.

small metal species (from monomeric to oligomeric and low-molecular-weight polymers) may only influence the kinetics and the stabilization of various metal species and intermediates during the hydrolysis event. At high [OH]/[Al] ratios, such effects will be further minimized because of the presence of larger metal species and stronger metal-coordinating hydroxides.

Considering that high viscosity and gel formation are the key criteria for antiperspirant action, the present work reveals the benefits of small Al species and the coparticipation of Zr(IV) and glycine, especially at lower pH values. These results are in good agreement with past findings, where the presence of acidic and monomeric Al was shown to be key for enhancing efficacy. However, the present study also reveals that the participation of small molecular species in cluster formation with larger species and complex formation with other components (e.g., glycine) could be critical for improving antiperspirant efficacy. As the present conclusions are not based on NMR data, they are not limited to symmetric and NMR-detectible species.[74] Furthermore, unlike in some recent studies, the gel was found to be the key mass in occlusive layer formation instead of the precipitate. Considering the high dependency of the hydrolysis event on the [OH]/[Al] ratio, the buffer capacity of the sweat current might also play a crucial role in determining the final local pH of the system. Thus, in a sweat current with a high buffer capacity, the sweat pH will be the determining factor. In this case, based on the present *in vitro* study, ACL and TETRA can be considered superior to the other investigated salt systems. However, if the sweat current has a lower buffer capacity and is unable to resist a local pH decrease, especially in the presence of highly acidic Al(III) salts, ACH, TRI, and OCTA would likely be more efficacious than predicted because the gel-forming pH would be achieved more rapidly. The present study not only offers unprecedented insights into the comparative hydrolysis events and associated chemistries of key and benchmark Al salts used in antiperspirant technology but also paves the way for system optimization by defining key criteria under more consumer-relevant conditions for the first time.

CONCLUSIONS

The hydrolysis chemistry of a series of Al(III) and/or Zr(IV) containing salts, including the benchmark ACL, which are frequently used as active ingredients in commercial antiperspirant products, was assessed in the pH range 4−7 using various rheological, spectroscopic, diffraction, analytical and imaging techniques. All of the tested systems formed gels at pH > 6, with TETRA and ACL also forming gels below pH 5. Unlike ACL, TETRA formed a transparent and slow-building gel only in the narrow pH range 4.5−5.0. Hydroxide formation and subsequent cluster formation aided by various small and polynuclear metal species were found to be responsible for gel formation above pH 6. The use of room-temperature hydrolysis and a short aging time (20 h) to replicate consumer-relevant conditions resulted in a wide distribution of various species and the formation of mostly amorphous gels. However, small Al and polynuclear Al species were found to be abundant in ACL and ACH, respectively, which were the most acidic and most basic salts. In contrast, the Al speciation of ZAG salts followed intermediate speciation patterns, depending on their acidity. In TETRA xerogels, the contribution from Zr(IV) was greater at lower pH values than at higher pH values. Similarly, the formation of metal−glycine complexes was found to be favorable at low pH values, whereas metal−hydroxide coordination became more favorable at high pH values. Small metal species with possible glycine coparticipation and metal−hydroxide coordination with the coparticipation of various polynuclear and oligomeric species were found to be the key factors for gel formation at low and high pH values, respectively. Parallel experiments in the model SM containing key sweat components revealed some effects on therheological behaviors. However, the effects of the sweat components were mostly limited to local complexation and the modification of hydrolysis kinetics and solubility. Moreover, these effects essentially disappeared at high pH values (>6). Based on the above findings, which were obtained under consumer-relevant conditions (ambient temperature and short aging time), ACL and TETRA are expected to be more efficacious than TRI, OCTA, and ACH. The present work, which is the first comprehensive and comparative *in vitro* study on Al and ZAG salts under consumer-relevant conditions, demonstrates for the first time that glycine may contribute to enhancing system efficacy and sheds light on the mechanism of action of widely used ZAG salts as the function of pH. In addition to addressing gaps in academic knowledge, the findings of this study will not only aid in the optimization of existing antiperspirant formulations for better efficacy but also motivate the development of alternative metal-free technologies.

ASSOCIATED CONTENT

Supporting Information

The Supporting Information is available free of charge at https://pubs.acs.org/doi/10.1021/acsami.1c22771.

Viscosity vs shear rate plots of 10% (w/v) ACL (Figure S1); viscosity vs shear rate plots of 10% (w/v) ACH (Figure S2); viscosity vs shear rate plots of 10% (w/v) TRI (Figure S3); viscosity vs shear rate plots of 10% (w/

https://doi.org/10.1021/acsami.1c22771
ACS Appl. Mater. Interfaces 2022, 14, 11597−11609

v) TETRA (Figure S4); viscosity vs shear rate plots of 10% (w/v) OCTA (Figure S5); FT-IR spectra of xerogel (Figure S6); and SEM images of xerogels (Figures S7–S9) (PDF)

AUTHOR INFORMATION

Corresponding Author

Harshita Kumari − *James L. Winkle College of Pharmacy, University of Cincinnati, Cincinnati, Ohio 45267-0004, United States;* orcid.org/0000-0002-6861-0281; Phone: +1-513-558-1872; Email: kumariha@ucmail.uc.edu

Authors

Arnab Dawn − *James L. Winkle College of Pharmacy, University of Cincinnati, Cincinnati, Ohio 45267-0004, United States;* orcid.org/0000-0002-9939-3240

Fred C. Wireko − *P&G Mason Business Center, Cincinnati, Ohio 45040, United States*

Andrei Shauchuk − *P&G Mason Business Center, Cincinnati, Ohio 45040, United States*

Jennifer L. L. Morgan − *P&G Mason Business Center, Cincinnati, Ohio 45040, United States;* orcid.org/0000-0002-6694-9687

John T. Webber − *P&G Mason Business Center, Cincinnati, Ohio 45040, United States*

Stevan D. Jones − *P&G Mason Business Center, Cincinnati, Ohio 45040, United States*

David Swaile − *P&G Mason Business Center, Cincinnati, Ohio 45040, United States*

Complete contact information is available at: https://pubs.acs.org/10.1021/acsami.1c22771

Notes

The authors declare no competing financial interest.

ACKNOWLEDGMENTS

The work was funded by Procter & Gamble.

REFERENCES

(1) Robinson, G. H. *Coordination Chemistry of Aluminum*; VCH, 1993.

(2) Berch, P. M. *The Environmental Chemistry of Aluminum*; Sposito, G., Ed.; CRC Press: Boca Raton, FL, 1989; p 87.

(3) Bi, S.; Wang, C.; Cao, Q.; Zhang, C. Studies on the Mechanism of Hydrolysis and Polymerization of Aluminum Salts in Aqueous Solution: Correlations Between the "Core-links" Model and "Cage-like" Keggin-Al_{13} Model. *Coord. Chem. Rev.* **2004**, *248*, 441–455.

(4) Hussain, S.; van Leeuwen, J.; Chow, C.; Beecham, S.; Kamruzzaman, M.; Wang, D.; Drikas, M.; Aryal, R. Removal of Organic Contaminants from River and Reservoir Waters by Three Different Aluminum-based Metal Salts: Coagulation Adsorption and Kinetics Studies. *Chem. Eng. J.* **2013**, *225*, 394–405.

(5) Zouboulis, A.; Traskas, G.; Samaras, P. Comparison of Efficiency Between Polyaluminium Chloride and Aluminium Sulphate Coagulants During Full-scale Experiments in a Drinking Water Treatment Plant. *Sep. Sci. Technol.* **2008**, *43*, 1507–1519.

(6) Zarchi, I.; Friedler, E.; Rebhun, M. Polyaluminium Chloride as an Alternative to Alum for the Direct Filtration of Drinking Water. *Environ. Technol.* **2013**, *34*, 1199–1209.

(7) Guo, T.; Chen, R.; Zhang, X.; Wu, J.; Wang, H.; Sun, Z. Stability, Morphological Transformation and Flocculability Investigation of Planar Tridecameric $Al_{13}(OH)_{24}(H2O)_{24}^{15+}$. *Sep. Purif. Technol.* **2017**, *184*, 288–297.

(8) Vicente, M. A.; Lambert, O. Al-pillared saponites Part 4, Pillaring with a New Al_{13} Oligomer Containing Organic Ligands. *Phys. Chem. Chem. Phys.* **1999**, *1*, 1633–1639.

(9) Occelli, M. L.; Bertrand, J. A.; Gould, S. A. C.; Dominguez, J. M. Physicochemical Characterization of a Texas Montmorillonite Pillared with Polyoxocations of Aluminum: Part I: The Microporous Structure. *Microporous Mesoporous Mater.* **2000**, *34*, 195–206.

(10) Wassberg, T. N.; Blaug, S. M.; Zopf, L. C. A Study of the Antibacterial Activity of Some Complex Aluminum Salts. *J. Am. Pharm. Assoc.* **1956**, *45*, 498–500.

(11) Londono, S. C.; Hartnett, H. E.; Williams, L. B. Antibacterial Activity of Aluminum in Clay from the Colombian Amazon. *Environ. Sci. Technol.* **2017**, *51*, 2401–2408.

(12) Savory, J.; Exley, C.; Forbes, W. F.; Huang, Y.; Joshi, J. G.; Kruck, T.; McLachlan, D. R.; Wakayama, I. Can the Controversy of the Role of Aluminium in Alzheimer's Disease be Resolved? What are the Suggested Approaches to This Controversy and Methodological Issues to be Considered? *J. Toxicol. Environ. Health* **1996**, *48*, 615–635.

(13) Darbre, P. D. Aluminium, Antiperspirants and Breast Cancer. *J. Inorg. Biochem.* **2005**, *99*, 1912–1919.

(14) Exley, C.; Burgess, E.; Day, J. P.; Jeffery, E. H.; Yokel, R. A. Aluminium Toxicokinetics. *J. Toxicol. Environ. Health* **1996**, *48*, 569–584.

(15) Perl, D. P.; Good, P. F. Uptake of Aluminium into Central Nervous System Along Nasal–Olfactory Pathways. *Lancet* **1987**, *329*, 1028–1029.

(16) Bondy, S. C. The Neurotoxicity of Environmental Aluminum is Still an Issue. *Neurotoxicology* **2010**, *31*, 575–581.

(17) IFSCC. Antiperspirants and Deodorants. In *Principles of Underarm Technology*; Monograph No 6; Micclle Press: Weymouth, MA, 1998.

(18) Schreiber, J. *Antiperspirant, Handbook of Cosmetic Science and Technology*, 2nd ed.; Marcel Dekker: New York, NY, 2005; pp 597–609.

(19) Cuzner, B.; Klepak, P. Antiperspirants and Deodorants. In *Poucher's Perfumes Cosmetics and Sops*, 9th ed.; Butler, H., Ed.; Chapman & Hall: London, 1933; Vol. 3, pp 3–26.

(20) Klepak, P. In vitro Killing Time Studies of Antiperspirant Salts. *SOFW* **1990**, *116*, 478–481.

(21) Rosenberg, A. Enhanced Efficacy Antiperspirant Actives. *Soap, Perfum. Cosmet.* **1997**, *7*, 27–30.

(22) Quatrale, R. P. The mechanism of Antiperspirant Action. *Cosmet. Toiletries* **1985**, *100*, 23–26.

(23) Laden, K.; Felger, C. B. *Antiperspirants and Deodorants: Cosmetic Science and Technology Series*; Marcel Dekker: New York, 1988; Vol. 7.

(24) Hözle, E.; Kligman, A. M. Mechanism of Antiperspirant action of aluminium salts. *J. Soc. Cosmet. Chem.* **1979**, *30*, 279–295.

(25) Quatrale, R. P.; Coble, D. W.; Stoner, K. L.; Felger, C. B. The Mechanism of Antiperspirant Action by Aluminiums Salts, II Histological Observations of Human Eccrine Sweat Glands Inhibited by Aluminium Chlorohydrate. *J. Soc. Cosmet. Chem.* **1981**, *32*, 107–136.

(26) Bretagne, A.; Cotot, F.; Arnaud-Roux, M.; Sztucki, M.; Cabane, B.; Galey, J.-B. The Mechanism of Eccrine Sweat Pore Plugging by Aluminium Salts Using Microfluidics Combined with Small Angle X-ray Scattering. *Soft Matter* **2017**, *13*, 3812–3821.

(27) Shen, Y. F. Enhanced Antiperspirant Salts Stabilized with Calcium and Concentrated Aqueous Solutions of Such Salts. U.S. Patent US6,245,325, 2001.

(28) Pan, L. Antiperspirant Active Compositions Having SEC Chromatogram Exhibiting High SEC Peak 4 Intensity. U.S. Patent US8,257,689, 2012.

(29) Ehlers, C.; Ivens, U. I.; Møller, M. L.; Senderovitz, T.; Serup, J. Females Have Lower Skin Surface pH than Men: A Study on the Influence of Gender, Forearm Site Variation, Right/Left Difference and Time of the Day on the Skin Surface pH. *Skin Res. Technol.* **2001**, *7*, 90–94.

(30) Patterson, M. J.; Galloway, S. D. R.; Nimmo, M. A. Variations in Regional Sweat Composition in Normal Human Males. *Exp. Physiol.* **2000**, *85*, 869−875.
(31) Harker, M.; Coulson, H.; Fairweather, I.; Taylor, D.; Daykin, C. A. Study of Metabolite Composition of Eccrine Sweat from Healthy Male and Female Human Subjects by ^{1}H NMR Spectroscopy. *Metabolomics* **2006**, *2*, 105−112.
(32) Herrmann, F.; Mandol, L. Studies of pH of Sweat Produced by Different Forms of Stimulation. *J. Invest. Dermatol.* **1955**, *24*, 225−246.
(33) Frink, C. R.; Beech, M. Hydrolysis of the Aluminum Ion in Dilute Aqueous Solutions. *Inorg. Chem.* **1963**, *2*, 473−478.
(34) Bottero, J. Y.; Tchoubar, D.; Cases, J. M.; Fiessinger, F. Studies of Hydrolyzed Aluminum Chloride Solutions. 1. Nature of Aluminum Species and Composition of Aqueous Solutions. *J. Phys. Chem. A* **1980**, *84*, 2933−2939.
(35) Fripiat, J. J.; Van Cauwelaert, F.; Bosmans, H. Structure of Aluminum Cations in Aqueous Solutions. *J. Phys. Chem. B* **1965**, *69*, 2458−2461.
(36) Brosset, C.; Wetlesen, C.-U.; Linholt, S. C.; et al. On the Reactions of Aluminum Ion with Water. *Acta Chem. Scand.* **1952**, *6*, 910−940.
(37) Sarpola, A.; Hellman, H.; Hietapelto, V.; Jalonen, J.; Jokela, J.; Ääämo, J.; Saukkoriipi, J. Hydrolysis Products of Water Treatment Chemical Aluminum Sulfate Octadecahydrate by Electrospray Ionization Mass Spectrometry. *Polyhedron* **2007**, *26*, 2851−2858.
(38) Casey, W. H. Large Aqueous Aluminum Hydroxide Molecules. *Chem. Rev.* **2006**, *106*, 1−16.
(39) Wang, D.; Sun, W.; Xu, Y.; Tang, H.; Gregory, J. Speciation Stability of Inorganic Polymer Flocculant−PACl. *Colloids Surf., A* **2004**, *243*, 1−10.
(40) Bottero, J. Y.; Axelos, M.; Tchoubar, D.; Cases, J. M.; Fripiat, J.; Fiessinger, J. F. Mechanism of Formation of Aluminum Trihydroxide from Keggin Al_{13} Polymers. *J. Colloid Interface Sci.* **1987**, *117*, 47−57.
(41) Zhao, H.; Liu, H.; Qu, J. Effect of pH On the Aluminum Salts Hydrolysis During Coagulation Process: Formation and Decomposition of Polymeric Aluminum Species. *J. Colloid Interface Sci.* **2009**, *330*, 105−112.
(42) Lydersen, E.; Salbu, B.; Poleo, A. B. S.; Muniz, I. P. The Influences of Temperature on Aqueous Aluminum Chemistry. *Water, Air, Soil Pollut.* **1990**, *51*, 203−215.
(43) XIAO, F.; ZHANG, B.; LEE, C. Effects of Low Temperature on Aluminum(III) Hydrolysis: Theoretical and Experimental Studies. *J. Environ. Sci.* **2008**, *20*, 907−914.
(44) Zhang, P.; Hahn, H. H.; Hoffmann, E.; Zeng, G. Influence of Some Additives to Aluminum Species Distribution in Aluminum Coagulants. *Chemosphere* **2004**, *57*, 1489−1494.
(45) Fu, G.; Nazar, L. F.; Bain, A. D. Aging Processes of Alumina Sol-Gels: Characterization of New Aluminum Polyoxycations by ^{27}A1 NMR Spectroscopy. *Chem. Mater.* **1991**, *3*, 602−610.
(46) Akitt, J. W.; Greenwood, N. N.; Khandelwal, B. L.; Lester, G. D. ^{27}Al Nuclear Magnetic Resonance Studies of the Hydrolysis and Polymerisation of the Hexa-aquo-aluminium(III) Cation. *J. Chem. Soc., Dalton Trans.* **1972**, 604−610.
(47) Singhal, A.; Keefer, K. D. A Study of Aluminum Speciation in Aluminum Chloride Solutions by Small angle X-ray Scattering and ^{27}Al NMR. *J. Mater. Res.* **1994**, *9*, 1973−1983.
(48) Thomas, F.; Maslon, A.; Bottero, J. Y.; Rouiller, J.; Montlgny, F.; Genévrler, F. Aluminum(III) Speciation with Hydroxy Carboxylic Acids. ^{27}Al NMR Study. *Environ. Sci. Technol.* **1993**, *27*, 2511−2516.
(49) Haouas, M.; Taulelle, F.; Martineau, C. Recent Advances in Application of (27)Al NMR Spectroscopy to Materials science. *Prog. Nucl. Magn. Reson. Spectrosc.* **2016**, *94*−*95*, 11−36.
(50) Chenyi, W.; Shuping, B.; Mingbiao, L. Review on the Progress of Analytical Methodologies for Polynuclear Aluminum in Environmental Water Systems. *Rev. Anal. Chem.* **2003**, *22*, 53−72.
(51) Ščančar, J.; Milačič, R. Aluminium Speciation in Environmental Samples: A Review. *Anal. Bioanal. Chem.* **2006**, *386*, 999−1012.
(52) Robmson, S.; Robmson, A. H. Chemical Composition of Sweat. *Physlol. Rev.* **1954**, *34*, 202−220.
(53) Fitzgerald, J. J. *Antiperspirants and Deodorants*; Laden, K.; Felge, C., Eds.; Dekker: New York, 1988; pp 119−291.
(54) Letterman, R. D.; Asolekar, S. R. Surface Ionization of Polynuclear Species in Al(III) hydrolysis—I. Titration Results. *Water Res.* **1990**, *24*, 931−939.
(55) Nail, S. L.; White, J. L.; Hem, S. L. Structure of Aluminum Hydroxide Gel I: Initial Precipitate. *J. Pharm. Sci.* **1976**, *65*, 1188−1191.
(56) Nail, S. L.; White, J. L.; Hem, S. L. Comparison of IR Spectroscopic Analysis and X-ray Diffraction of Aluminum Hydroxide Gel. *J. Pharm. Sci.* **1975**, *64*, 1166−1169.
(57) Gwett, T.; de Navarre, M. G. Aluminum Chlorohydrate, New Antiperspirant Ingredient. *Am. Perfum. Ess. Oil Rev.* **1947**, *49*, 365.
(58) Shefter, E.; Giannini, R. P. Hydrolytic Behavior of Some Aluminum Antiperspirant Materials in Acid. *Int. J. Pharm.* **1978**, *1*, 49−59.
(59) Phillips, B. L.; Vaughn, J. S.; Smart, S.; Pan, L. Characterization of Al_{30} in Commercial Poly-Aluminum Chlorohydrate by Solid-state ^{27}Al NMR Spectroscopy. *J. Colloid Interface Sci.* **2016**, *476*, 230−239.
(60) Teagarden, D. L.; White, J. L.; Hem, S. L. Aluminum Chlorohydrate III: Conversion to Aluminum Hydroxide. *J. Pharm. Sci.* **1981**, *70*, 808−810.
(61) Allouche, L.; Taulelle, F. Conversion of Al_{13} Keggin ε into Al_{30}: A Reaction Controlled by Aluminum Monomers. *Inorg. Chem. Commun.* **2003**, *6*, 1167−1170.
(62) Teagarden, D. L.; Kozlowski, J. F.; White, J. L.; Hem, S. L. Aluminum Chlorohydrate I: Structure Studies. *J. Pharm. Sci.* **1981**, *70*, 758−761.
(63) Nail, S. L.; White, J. L.; Hem, S. L. IR Studies of Development of Order in Aluminum Hydroxide Gels. *J. Pharm. Sci.* **1976**, *65*, 231−234.
(64) Bradley, S. M.; Kydd, R. A.; Howe, R. F. The Structure of Al Gels Formed through the Base Hydrolysis of Al^{3+} Aqueous Solutions. *J. Colloid Interface Sci.* **1993**, *159*, 405−412.
(65) Leetmaa, K.; Gomez, M. A.; Becze, L.; Guo, F.; Demopoulos, G. P. Comparative Molecular Characterization of Aluminum Hydroxy-gels Derived from Chloride and Sulphate Salts. *J. Chem. Technol. Biotechnol.* **2014**, *89*, 206−213.
(66) Bollino, F.; Armenia, E.; Tranquillo, E. Zirconia/Hydroxyapatite Composites Synthesized Via Sol-Gel: Influence of Hydroxyapatite Content and Heating on Their Biological Properties. *Materials* **2017**, *10*, 757.
(67) Hao, Y.; Li, J.; Yang, X.; Wang, X.; Lu, L. Preparation of ZrO_2−Al_2O_3 Composite Membranes by Sol−Gel Process and their Characterization. *Mater. Sci. Eng., A* **2004**, *367*, 243−247.
(68) Nazar, L. F.; Klein, L. C. Early Stages of Alumina Sol-Gel Formation in Acidic Media: An ^{27}Al Nuclear Magnetic Resonance Spectroscopy Investigation. *J. Am. Ceram. Soc.* **1988**, *71*, C85−C87.
(69) Kiss, T.; Sóvágó, I.; Tóth, I.; Lakatos, A.; Bertani, R.; Tapparo, A.; Bombi, G.; Martin, R. B. Complexation of Aluminium(III) with Several bi- and tri-Dentate Amino Acids. *J. Chem. Soc., Dalton Trans.* **1997**, 1967−1972.
(70) Deschaume, O.; Breynaert, E.; Radhakrishnan, S.; Kerkhofs, S.; Haouas, M.; de Beaumais, S. A.; Manzin, V.; Galey, J.-B.; Ramos-Stanbury, L.; Taulelle, F.; Martens, J. A.; Bartic, C. Impact of Amino Acids on the Isomerization of the Aluminum Tridecamer Al_{13}. *Inorg. Chem.* **2017**, *56*, 12401−12409.
(71) Wang, S.; Wahiduzzaman, M.; Davis, L.; Tissot, A.; Shepard, W.; Marrot, J.; Martineau-Corcos, C.; Hamdane, D.; Maurin, G.; Devautour-Vinot, S.; Serre, C. A Robust Zirconium Amino Acid Metal-Organic Framework for Proton Conduction. *Nat. Commun.* **2018**, *9*, No. 4937.
(72) Yao, H.-B.; Yan, Y.-X.; Gao, H.-L.; Vaughn, J.; Pappas, I.; Masters, J. G.; Yuan, S.; Yu, S.-H.; Pan, L. An Investigation of Zirconium(IV)−Glycine(CP-2) Hybrid Complex in Bovine Serum Albumin Protein Matrix Under Varying Conditions. *J. Mater. Chem.* **2011**, *21*, 19005−19012.

https://doi.org/10.1021/acsami.1c22771
ACS Appl. Mater. Interfaces 2022, 14, 11597−11609

(73) Further studies on glycine-metal complexation as the function of pH under ambient conditions and associated hydrolysis and speciation chemistry is currently undergoing and will be published separately.
(74) A detailed NMR studies on various Al and ZAG salts and glycine involvement in the pH range 4−7 are in progress and will be published separately.

https://doi.org/10.1021/acsami.1c22771
ACS Appl. Mater. Interfaces 2022, 14, 11597−11609